Macromolecules

Article

pubs.acs.org/Macromolecules

Biaxially Extended Quaterthiophene− and Octithiophene−Vinylene Conjugated Polymers for High Performance Field Effect Transistors and Photovoltaic Cells

Chien Lu,† Hung Chin Wu,† Yu Cheng Chiu, Wen Ya Lee, and Wen Chang Chen*

Department of Chemical Engineering, National Taiwan University, Taipei, Taiwan 10617

Supporting Information

ABSTRACT: We report the synthesis, morphology, and optoelectronic device applications of novel biaxially extended quaterthiophene− (**4T**−) and octithiophene− (**8T**−) vinylene conjugated polymers, **P4TV** and **P8TV**, synthesized via Stille coupling reactions. **P4TV** and **P8TV** exhibited smaller energy band gaps of 1.69 and 1.78 eV than that of parent polythiophenes, respectively, due to the reduced conformation distortion by the vinylene linkage. The HOMO energy levels of **P4TV** and **P8TV** were −5.02 and −5.13 eV, respectively, resulting in air stable device performance. The highest field effect hole mobilities of **P4TV** and **P8TV** were 0.12 and 0.0018 $cm^2\ V^{-1}\ s^{-1}$, respectively, with on/off ratios around 10^4−10^5. The higher carrier mobility of **P4TV** was related to its ordered structure as evidenced from the TEM, AFM, and grazing incidence X-ray diffraction results. The power conversion efficiency (PCE) of the **P4TV**/ $PC_{71}BM$ based photovoltaic cells (PV) under the illumination of AM 1.5G (100 mW/cm^2) was 4.04%, which was significantly higher than that of **P8TV**/$PC_{71}BM$ with 2.69%, due to its superior charge transport ability. However, **P8TV** had a better environmental stability attributed to its low-lying HOMO energy level. These above results demonstrate that biaxially extended thiophene−vinylene conjugated copolymers could be promising materials for high performance organic electronic device applications.

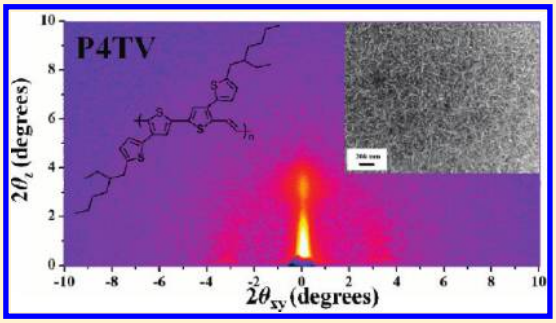

INTRODUCTION

Conjugated polymers have been intensively developed recently for applications in organic electronics such as light-emitting diodes,[1,2] field effect transistors (FETs),[3−8] photovoltaic cells (PVs),[9−17] and memory devices.[18−20] Among these polymers that used in electronic devices, polythiophenes have been attracted large interest due to their essential solubility, processability, and judicious structural flexibility.[21] Regioregular poly(3-hexylthiophene) (P3HT), one of the well-documented conjugated polymers, showed high hole mobilities in range of 0.05−0.2 $cm^2\ V^{-1}\ s^{-1}$[22−24] and PV cells efficiencies around 4−5%.[9,25−27] However, the relatively high HOMO levels obstruct the environmental stability for device applications.[28]

One approach toward high-performance FET or PV devices is the use of highly coplanar conjugated polymers with effective conjugation length and compact molecular packing. Poly(thienylene vinylene)s (PTVs) with a highly coplanar backbone exhibited a low band gap (1.55−1.64 eV) and ordered structure, since the vinylene linkage could reduce the steric hindrance.[29−37] However, the poor solubility of PTV limited their practical device applications.[29,30] Recently, several PTV derivatives were reported for high charge carrier mobility.[31−35] Kim and his co-workers reported low-band gap PC6TV12T with the hole mobility up to 1.05 $cm^2\ V^{-1}\ s^{-1}$, attributed to the coplanar TV unit.[36] However, despite of the low band gaps of PTVs, the power conversion efficiency (PCE) of the PV cells was low (0.24−1.2%).[32−34,37] To further improve the performance of PTV based optoelectronic devices, it is important to design new polymers with high charge carrier mobility, broad absorption in visible region, and optimized morphology.[28,38,39]

Biaxially extended conjugated polymers[40−47] were reported to enhance the absorption range and the carrier mobility for device applications, due to the extension of π-electron delocalization. Li and co-workers reported that the incorporation of conjugated side chains into thiophene backbone facilitated the extension of π-electron delocalization and have broad absorption, such as bi(thienylenevinylene),[38,40] bi(phenylenevinylene),[41] and phenothiazinevinylene.[48] We discovered the biaxial extended conjugated thiopohene-acceptor or fused thiophene copolymers with high unipolar or ambipolar carrier mobility (3×10^{-4} to 0.61 $cm^2\ V^{-1}\ s^{-1}$).[28,41−43] Also, the relatively low-lying HOMO levels (−5.04 to −5.62 eV)[28,43−45] could enhance the open-circuit voltage for high performance PV applications. On the other hand, dendritic and branched thiophenes derivatives were reported to improve charge transport,[49−52] processing solubility,[53,54] or compatibility with PCBM molecules.[39] Thus, conjugated polymers with branched conjugated side chains would be potential candidates for optoelectronic device applications owing to good charge transport, broad absorption, and high air stability.

Received: February 15, 2012
Revised: March 17, 2012
Published: March 26, 2012

Scheme 1. Synthetic Route on Preparing P4TV and P8TV

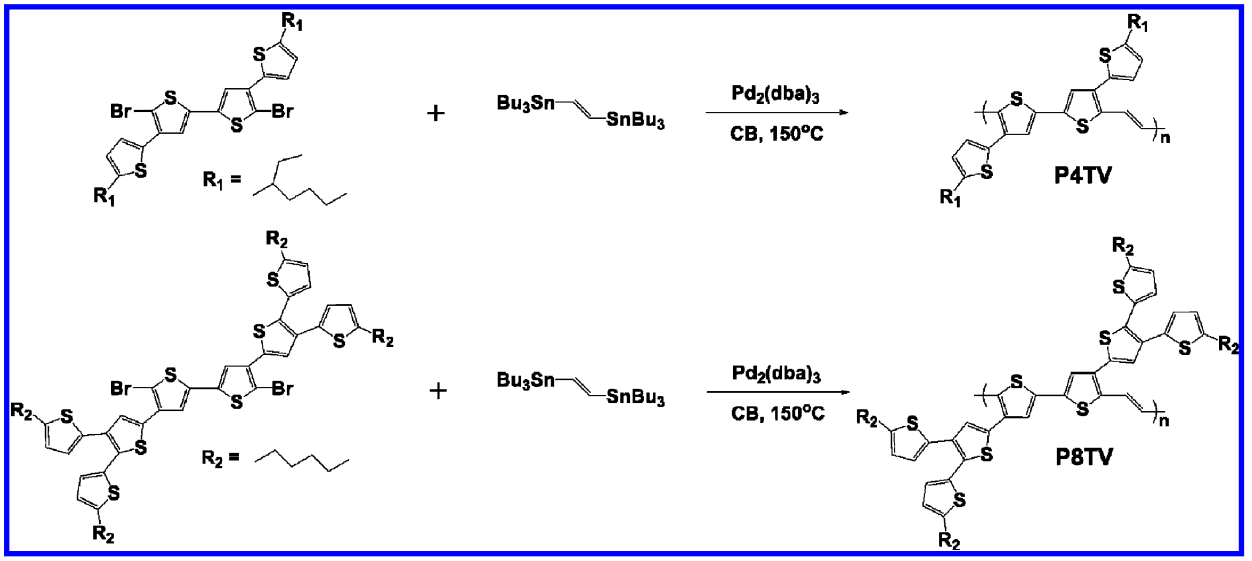

In this paper, we report the synthesis, morphology, and device applications of new biaxially extended conjugated (thiophene-vinylene), poly[(*E*)-5,5‴-bis(2-ethylhexyl)-2′-methyl-5″-(prop-1-en-1-yl)-2,3′:5′,2″:4″,2‴-quaterthiophene] (**P4TV**) and poly[(*E*)-5,5⁗-dihexyl-3′,5‴-bis(5-hexylthiophen-2-yl) −5‴-methyl-2″-(prop-1-en-1-yl)-2,2′:5′,3″:5″,2‴:4‴,2⁗:4⁗,2⁗⁗:4⁗⁗,2⁗⁗⁗-sexithiophene] (**P8TV**). The incorporation of the vinylene unit into the biaxially extended quaterthiophene (**4T**) and octithiophene (**8T**) could enhance the backbone coplanarity to improve charge transport characteristics for device applications. Furthermore, the branched conjugated thiophene side chain may have a broad absorption for enhance PV performance. **P4TV** and **P8TV** were synthesized by Stille coupling reaction under microwave heating, as shown in Scheme 1. The morphology of the prepared conjugated polymers was investigated by transmission electron microscopy (TEM), atomic force microscopy (AFM), and grazing incidence X-ray diffraction (GIXD) analysis. The charge carrier mobility was obtained from the top-contact/bottom-gate field effect transistor device structure. Moreover, the photovoltaic cell with device structure of ITO/PEDOT:PSS/polymer:$PC_{71}BM$/Ca/Al using **P4TV** and **P8TV** were fabricated and characterized.

EXPERIMENTAL SECTION

Materials. Tri(*o*-tolyl)phosphine, tris(dibenzylideneacetone)-dipalladium(0), trimethyl(thiophen-2-yl)stannane, and bromothiophene were purchased from Aldrich (Missouri) and used without further purification. P3HT (M_w ∼ 50 000 g/mol, 90−95% regioregular) was used as received from Reike Metals Inc. (Lincoln, NE). Common organic solvents for synthesis were distilled to keep anhydrous or degassed by nitrogen 0.5 h before using. Ultra-anhydrous *o*-dichlorobenzene for device applications was purchased from Aldrich (Missouri). The monomer of 2′,5″-dibromo-5,5‴-di- (2-ethylhexyl)-[2,3′;5′,2″;4″,2‴]quaterthiophene (**4T-Br$_2$**) was synthesized according to our previous work.[43,45] The synthesis of 2″,5‴-dibromo-5,5⁗-dihexyl-3′,5‴-bis(5-hexylthiophen-2-yl)-2,2′:5′,3″:5″,2‴:4‴,2⁗:4⁗,2⁗⁗:4⁗⁗,2⁗⁗⁗-sexithiophene (**8T-Br$_2$**) is shown in the Supporting Information. A surface treatment agent of octadecyltrichlorosilane (ODTS) was purchased from Acros (Geel, Belgium) for field-effect transistor characterization. [6,6]-phenyl-C71-butyric acid methyl ester ($PC_{71}BM$) was purchased from Solenne BV (Groningen, The Netherlands) for photovoltaic cell applications.

General Procedures for Polymerization. The general procedure of synthesizing **P4TV** and **P8TV** is shown in Scheme 1. (*E*)-1,2-Bis(tributylstannyl)ethylene (**V-ditin**), dibromomonomers (**4T-Br$_2$** and **8T-Br$_2$**), tri(*o*-tolyl)phosphine (16 mol % with respect to ditin monomer), and tris(dibenzylideneacetone)dipalladium(0) (2 mol % with respect to ditin monomer) were dissolved in chlorobenzene. Then, these copolymers were synthesized by Pd(0)-catalyzed Stille coupling polymerization under microwave heating (150 °C for 30 min). After end-capped with trimethyl(thiophen-2-yl)stannane and bromothiophene (both 1.1 equiv with respect to the monomers and under microwave heating at 160 °C for 10 min on the end-capping), the mixture was cooled and poured into methanol to afford a crude solid. The crude polymer was purified by methanol, acetone and hexane successively using a Soxhlet extraction to remove byproducts, oligomers and catalyst residues.

*Poly[(E)-5,5‴-bis(2-ethylhexyl)-2′-methyl-5″-(prop-1-en-1-yl)-2,3′:5′,2″:4″,2‴ -quaterthiophene] (**P4TV**).* Amounts of 284.02 mg (0.40 mmol) of **4T-Br$_2$**, 242.46 mg (0.40 mmol) of **V-ditin**, and 15 mL of chlorobenzene were used to afford a purple solid (yield, 65%). ^{1}H NMR (CD_2Cl_2), δ (ppm): 7.51−6.19 (m, br, Ar−H and Vin-H, 8H), 2.15−1.72 (br, Ar−CH_2, 4H), 1.49−1.15 (br, −CH and −CH_2, 18H), 1.15−0.46 (br, −CH_3, 12H). Anal. Calcd for [$C_{32}H_{44}S_4$]: C, 70.29; H, 7.63 S, 22.08. Found: C, 68.62; H, 7.01; S, 21.90. Weight-average molecular weight (M_w) and polydispersity index (PDI) estimated from GPC are 87025 g/mol and 2.51, respectively.

*Poly[(E)-5,5⁗-dihexyl-3′,5⁗⁗-bis(5-hexylthiophen-2-yl)-5‴-methyl-2″-(prop-1-en-1-yl)-2,2′:5′,3″:5″,2‴:4‴,2⁗:4⁗⁗,2⁗⁗⁗-sexithiophene] (**P8TV**).* Amounts of 460.04 mg (0.40 mmol) of **8T-Br$_2$**, 242.46 mg (0.40 mmol) of **V-ditin**, and 15 mL of chlorobenzene were used to afford a black solid (yield, 68%). ^{1}H NMR (CD_2Cl_2), δ (ppm): 7.61−6.19 (m, br, Ar−H and Vin-H, 14H), 2.90−2.31 (br, Ar−CH_2, 8H), 1.49−0.97 (m, br, −CH_2, 32H), 0.97−0.58 (m, br, −CH_3, 12H). Anal. Calcd for [$C_{58}H_{66}S_8$]: C, 68.18; H, 6.71 S, 25.11. Found: C, 67.76; H, 6.28; S, 25.33. Weight-average molecular weight (M_w) and polydispersity index (PDI) estimated from GPC are 59630 g/mol and 2.33, respectively.

Characterization. Microwave reaction was carried out using a Biotage microwave reactor in sealed vessels. ^{1}H NMR spectra were recorded with a Bruker Avance DRX 400 MHz instrument. Gel permeation chromatographic (GPC) analysis was performed on a Lab Alliance RI2000 instrument (two column, MIXED-C and -D from Polymer Laboratories) which was connected to one refractive index detector from Schambeck SFD Gmbh. All GPC analyses were performed on polymer/THF solution at a flow rate of 1 mL/min at 40 °C and calibrated with polystyrene standards. Thermogravimetric analysis (TGA) and differential scanning calorimetry (DSC) measurements were performed under a nitrogen atmosphere at a heating rate

dx.doi.org/10.1021/ma300313y | *Macromolecules* 2012, 45, 3047−3056

of 10 °C/min by using the TA Instruments Q-50 and Q-100, respectively. X-ray diffraction patterns were collected by X-ray scattering in a grazing-incidence geometry (Nano-Viewer, Rigaku) that includes a two-dimensional (2D) area detector (Rigaku, 100 K PILATUS). The instrument is equipped with a 31 kW mm^{-2} generator (rotating anode X-ray source with a Cu Ka radiation of λ = 0.154 nm). The scattering vector, q ($q = 4\pi/\lambda[\sin\theta]$), along with the scattering angles q in these patterns were calibrated using silver behenate. The thin films were mounted on a z-axis goniometer. UV−visible absorption spectra were recorded using a Hitachi U-4100 spectrophotometer. For the thin film spectra, polymers were first dissolved in o-dichlorobenzene, followed with filtering through a 0.45 μm pore size PTFE membrane syringe filter, and then spin-coated at a speed rate of 800 rpm for 60 s onto quartz substrate. The absorption coefficients were calculated using the Beer's law, and the film thickness was determined with a Microfigure Measuring Instrument (Surfcorder ET3000, Kosaka Laboratory Ltd.). Cyclic voltammetry (CV) was recorded on a CHI 611B electrochemical analyzer using the use of a three-electrode cell in which ITO (polymer films area were about 0.5 × 0.7 cm^2) was used as a working electrode. A platinum wire was used as an auxiliary electrode. All cell potentials were taken with the use of a homemade Ag/AgCl, KCl (sat.) reference electrode. The electrochemical properties of the polymer films were detected under 0.1 M anhydrous acetonitrile solution containing tetrabutylammonium perchlorate (TBAP) as electrolyte. The morphology of polymer film surface was obtained with a Nanoscope 3D Controller atomic force micrographs (AFM, Digital Instruments) operated in the tapping mode at room temperature. Transmission electron microscopy (TEM) images were obtained with a JEOL JEM-1230 instrument operating at a voltage of 100 kV with a Gatam dual vision CCD camera. For the measurements of GIXD, UV, AFM, and TEM, the preparation of polymer samples were the same with that of the device fabrication.

Computational Methodology. Theoretical molecular simulation of the studied polymers was calculated through Gaussian 03 program package.[55] Density functional theory (DFT) method, using Becke's three-parameter functional with the Lee, Yang, and Parr correlation functional method (B3LYP) with 6-31G(d), was used for the optimization of ground-state molecular geometry.

Fabrication and Characterization of Field Effect Transistors. Highly doped n-type Si(100) wafers were used as substrates. A 200 nm SiO_2 layer (capacitance per unit area C_o = 17 nF cm^{-2}) as a gate dielectric was thermally grown onto the Si substrates. These wafers were cleaned in piranha solution (Caution!), a 7:3 (v/v) mixture of H_2SO_4 and H_2O_2, rinsed with deionized water, and then dried by N_2. The octadecyltrichlorosilane (ODTS)-treated surfaces on SiO_2/Si substrates were obtained by the following procedure: a clean SiO_2/Si substrate was immersed into a 10 mM solution of trichlorosilane in toluene at 80 °C for 2 h. Then the substrates were rinsed with toluene and dried with a steam of nitrogen. FET devices were fabricated by spin-coating of the polymer solution in o-dichlorobenzene (12 mg/mL) at a spin rate of 800 rpm for 60 s, and annealed at 100 °C for 60 min. The top-contact source and drain electrodes were defined by 100 nm-thick gold through a regular shadow mask, and the channel length (L) and width (W) were 50 and 1000 μm, respectively. FET transfer and output characteristics were recorded in a N_2-filled glovebox or in ambient by using a Keithley 4200 semiconductor parametric analyzer.

Fabrication and Characterization of Polymer Photovoltaic Cells. All the bulk heterojunction photovoltaic cell was fabricated through the following preparation procedures: The glass−indium tin oxide (ITO) substrate (obtained from Lumtec, (7 Ω/sq)) was first patterned by lithograph, then cleaned with detergent, and ultrasonicated in acetone and isopropyl alcohol, and subsequently dried on a hot plate at 120 °C for 5 min, and finally treated with oxygen plasma for 5 min. Poly(3,4-ethylenedioxy−thiophene):poly(styrene−sulfonate) (PEDOT:PSS, Baytron P VP AI4083) was passed through a 0.45 μm filter and then spin-coated at 5000 rpm on ITO in air and dried at 140 °C for 20 min inside the glovebox. The polymer/$PC_{71}BM$ blend was prepared by dissolving them in anhydrous o-dichlorobenzene (18 mg/mL) followed by spin-coating on the top of the PEDOT:PSS layer. The device was then annealed at 100 °C for 10 min (**P4TV** and **P8TV**) or 140 °C for 20 min (P3HT) in glovebox. Subsequently, the device was deposited with a 30 nm thickness of Ca and a 100 nm thickness of Al by thermal evaporation under high vacuum (<10^{-6} Torr), respectively. The active area of the device is 4 mm^2. The current−voltage (J−V) measurement of the polymer photovoltaic cell was conducted by a computer-controlled Keithley 2400 source measurement unit (SMU) with a Peccell solar simulator under the illumination of AM 1.5 G, 100 mW/cm^2. The illumination intensity was calibrated by a standard Si photodiode detector with KG-5 filter.

RESULTS AND DISCUSSION

Polymer Characterization. The chemical structures of the synthesized polymers were confirmed by ^{1}H NMR and elemental analysis. Figure 1 shows the ^{1}H NMR of **P4TV**

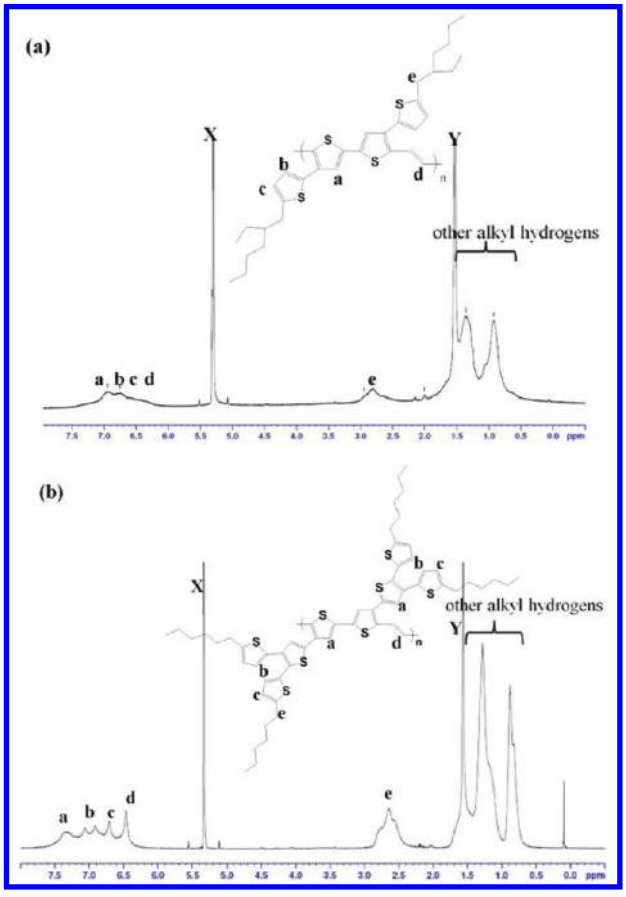

Figure 1. ^{1}H NMR spectra of (a) **P4TV** and (b) **P8TV** in CD_2Cl_2. (X, CD_2Cl_2; Y, H_2O).

and **P8TV** in CD_2Cl_2. For the spectrum of **P4TV**, the three peaks at 7.01 (peak a), 6.75 (peak b), and 6.56 (peak c) ppm are assigned to the aromatic protons on the thiophene rings of the 4T unit, while the peak at 6.32 (peak d) ppm is attributed to the proton on the vinylene segment. Moreover, the peaks at 2.15−1.72 ppm (thiophene−CH_2, peak e), 1.49−1.15 ppm (−CH and −CH_2), and 1.15−0.46 ppm (−CH_3) are attributed to the ethylhexyl group in the 4T unit, respectively. Similarly, the chemical shift and proton numbers in the NMR spectrum of **P8TV** is also consisted with the proposed structure. The elemental carbon, hydrogen, and sulfur contents of the studied polymers are in a good agreement with the theoretical content. The above results suggest the successful preparation of the biaxially extended thiophene−vinylene conjugated polymers.

dx.doi.org/10.1021/ma300313y | Macromolecules 2012, 45, 3047−3056

Both **P4TV** and **P8TV** have good solubility in common chlorinated solvents and thus could be spin-coated into optical quality films for device applications, including chloroform, chlorobenzene, and *o*-dichlorobenzene. The weight-averaged molecular weight and the polydispersity index (M_w, PDI) of **P4TV** and **P8TV** estimated by GPC (Figure S2 of Supporting Information) using polystyrene standards in THF are (87025, 2.51) and (59630, 2.33), respectively.

The thermal properties of **P4TV** and **P8TV** were evaluated by thermo-gravimetric analysis (TGA) and differential scanning calorimetry (DSC) as shown in Figure S3 (Supporting Information). The thermal decomposition temperature (T_d) values of **P4TV** and **P8TV** are 392 and 408 °C, respectively, indicating their good thermal stability. DSC curves were measured up to 250 °C, but no obvious thermal transition in the bulk sample was observed.

Optical Properties. The UV−visible absorption spectra of **P4TV** and **P8TV** thin films are shown in Figure 2a, and

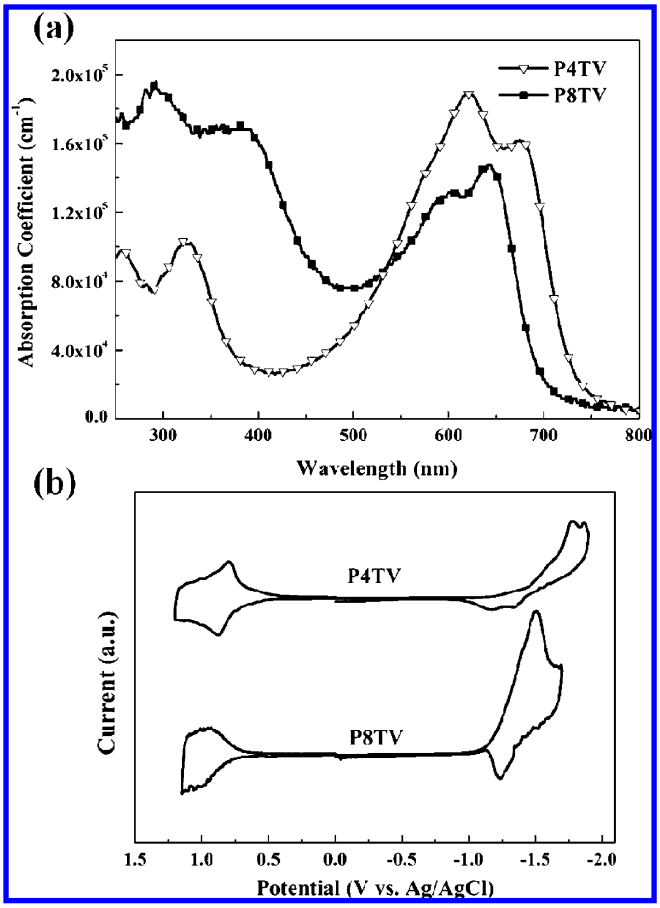

Figure 2. (a) Optical absorption spectra of the **P4TV** and **P8TV** thin films on a quartz plate. (b) Cyclic voltammograms of the **P4TV** and **P8TV** thin film in an acetonitrile solution of 0.1 M TBAP at a scan rate of 100 mV/s.

summarized in Table 1. The absorption maximum wavelength (λ_{max}) in the visible region of the **P4TV** and **P8TV** thin films are observed at 621 and 675 nm for **P4TV** and 603 and 643 nm for **P8TV**, respectively, attributed to the $\pi-\pi^*$ electronic transition. The λ_{max} of the two polymers in dilute *o*-dichlorobenzene (Figure S4 of Supporting Information) are similar to those of the thin films. Both **P4TV** and **P8TV** thin films possess an absorption peak with a clearly observed shoulder, indicating the higher structural organization and ordered packing. The E_g^{opt} of **P4TV** and **P8TV** estimated from the absorption edge are 1.69 and 1.78 eV, respectively, which are smaller than the P3HT with 1.8−2.0 eV. It again suggests the importance of the vinylene linkage affecting the backbone coplanarity and the resulted band gap. **P8TV** has a more branched thiophene side chains and thus provides a higher rotation freedom, leading to reduce the effective conjugation length for a higher E_g than that of **P4TV**.[56] Compare to those P3HT and PTVs, the absorption peaks of **P4TV** (λ_{max} = 325 nm) and **P8TV** (λ_{max} = 291 and 391 nm) located in ultraviolet region arise from the $\pi-\pi^*$ transition of conjugated side chains.[40] Obviously, the relatively branched thiophene of **P8TV** exhibit a higher absorption intensity in the ultraviolet region than that of **P4TV**.

Figure 3 is the optimized geometry on the dimers of **P4TV** and **P8TV**, calculated at the B3LYP/6-31G(d) level through Gaussian 03 program package. θ_α and θ_γ are the torsional angles of the dimers in the main chain, and θ_β and θ_ω are torsional angles of the dimers in the side chains. The small main-chain torsional angles (θ_α, θ_γ) are (1.6°, 4.5°) and (8.5°, 10.2°) for **P4TV** and **P8TV**, respectively, which are smaller than that of P4T (18°, 84°) in our previous work.[45] It indicates that the vinylene moieties inserted into biaxially extended conjugated polythiophene significantly reduces the torsion within the main chain. Besides, **P4TV** exhibit a higher degree of coplanarity than **P8TV**. The side-chain torsional angles (θ_β) are 41.3° and 39.3° for **P4TV** and **P8TV**, respectively. The side-chain torsional angles of branched thiophenes of **P8TV** are 39.6−49.5°, suggesting higher rotational freedom of the branched thiophene side chains. The structural conformation result of **P4TV** and **P8TV** is consistent with the optical band gap described in the previous section. Besides, the optical band gap of **P4TV** is lower compared to other **4T**-based conjugated polymers (1.80−2.65 eV).[37,38] The broad absorption characteristic could also improve the PV cell characteristics and elevate the photocurrent spectrum.

The thin films of **P4TV** (1.89×10^5 cm^{-1} at ca. 621 nm) and **P8TV** (1.47×10^5 cm^{-1} at ca. 643 nm) exhibit moderate absorption coefficients comparable to that of the P3HT film (1.9×10^5 cm^{-1} at ca. 552 nm).[57] The high absorption coefficient of **P4TV** suggests its potential to enhance the PV cells performance.

Electrochemical Properties. The electrochemical characteristics measured in acetonitrile at potential scan rate of 100 mV/s are shown in Figure 2b and summarized in Table 1. The highest occupied molecular orbital (HOMO) energy level, the lowest unoccupied molecular orbital (LUMO) energy level, and the electrochemical band gap (E^{ec}_g) were estimated from the onset oxidation potential (E^{ox}_{onset}) and onset reduction potential (E^{red}_{onset}), based on the following equations: HOMO = $-[E^{ox}_{onset} - E^{ferrocene}_{1/2} + 4.8]$ V; LUMO = $-[E^{red}_{onset} - E^{ferrocene}_{1/2} + 4.8]$ V, where the potential is referred to an Ag/AgCl reference electrode. Apparently, both polymers exhibit both reversible oxidation and reduction processes. The corresponding HOMO energy levels of **P4TV** and **P8TV** are −5.02 and −5.13 eV, respectively, while their LUMO energy levels are −3.15 and −3.16 eV. The corresponding electrochemical band gaps of **P4TV** and **P8TV** are 1.87 and 1.97 eV. The higher HOMO level of **P4TV** than that of **P8TV** is attributed the better backbone coplanarity of the former. Moreover, the HOMO energy levels of **P4TV** and

dx.doi.org/10.1021/ma300313y | *Macromolecules* 2012, 45, 3047−3056

Table 1. Optical and Electrochemical Properties of P4TV and P8TV

	optical absorption				cyclic voltammetry		
polymer	λ_{max}(sol)[a] (nm)	λ_{max}(film)[a] (nm)	α[b] ($\times 10^5$ cm^{-1})	E_g^{opt} (eV)	E^{ox}_{onset}/HOMO (V/eV)	E^{red}_{onset} /LUMO (V/eV)	E_g^{ec} (eV)
P4TV	325, 622, 677	325, 621, 675	1.89	1.69	0.70/−5.02	−1.17/−3.15	1.87
P8TV	380, 592. 638	391, 603, 643	1.47	1.78	0.81/−5.13	−1.16/−3.16	1.97

[a] *o*-dichlorobenzene as processing solvent. [b] Absorption coefficient (α) of the solid thin film at its maximum peak intensity in the visible region (420−700 nm) ($\times 10^{-5}$ cm^{-1}).

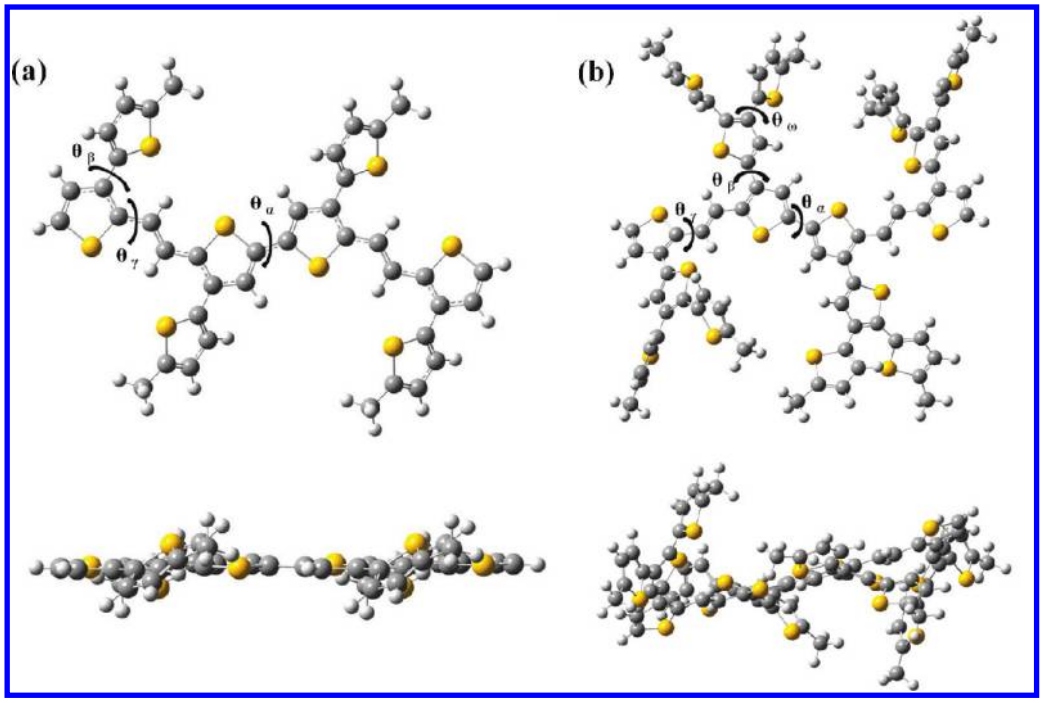

Figure 3. Optimized backbone structure of (a) **P4TV** and (b) **P8TV** in 2 units. The side chains were replaced with the methyl groups to simplify the calculation.

P8TV are lower than P3HT (−4.90 eV), indicating these polymers could have better air stability.

Morphology Characterization. The film morphology of **P4TV** and **P8TV** were examined using Transmission electron microscopy (TEM), atomic force microscopy (AFM), and grazing incidence X-ray diffraction (GIXD) analyses. Figure 4 shows TEM images of the thermal annealed **P4TV** and **P8TV** thin films. The annealed **P4TV** thin film showed a more organized nanofirbrillar structure as compared to **P8TV**. The well-ordered morphology of **P4TV** was expected to result in good charge carrier transporting characteristics. The thin film morphology of **P8TV** was nearly amorphous because the bulky pendent branched thiophene moiety reduces the ordering of polymer backbones. As shown in Figure 5, GIXD analyses of annealed thin films (thickness of 40−50 nm) were carried out to further investigate the structural ordering. The primary diffraction patterns of **P4TV** (Figure 5a) and **P8TV** (Figure 5b) are observed at $2\theta_z$ = 3.66 and 4.06°, respectively, corresponding to the *d*-spacing of 24.14 and 21.76 Å, respectively. The diffraction intensity of **P4TV** is markedly stronger than **P8TV**. It is consistent with the appearance of orderly nanofirbrillar structure of **P4TV** in the TEM images. In Figure 5c, the full width half-maximum (fwhm) of the azimuthal-angle intensity of the first order diffraction is estimated to be 9.49 and 20.25° for **P4TV** and **P8TV**. It suggests that **P4TV** has a significantly concentrative orientation distribution of the crystalline domains with respect to the substrate surface. The alignment of **P4TV** is also more concentrative than that broader orientation distribution of P3HT (fwhm = 14.1° for the best condition).[58] Besides, the *d*-spacing of the studied polymers are slightly larger than that of the other PTVs reported in the literature.[36] Also, P4T also showed a smaller *d*-spacing (16.8 Å) in our previous work.[45] The above results suggest the side chains on the thiophenes and vinylene moieties truly affect the interdigitation of polymer backbones. Furthermore, the nanofirbrillar morphology of **P4TV** was also observed in tapping mode AFM phase images (Figure S5 of Supporting Information)). The ordering nanofirbrillar structure of **P4TV** film with the interconnected networks of the polymer chains may provide the formation of highly efficient pathways for charge carrier transport.[58,59]

Polymer Field-Effect Transistor (FET) Characteristics. Solution-processed top contact FETs based on **P4TV** and **P8TV** were fabricated from *o*-dichlorobenzene. Figure 6 shows the FET transfer characteristics of the copolymer devices on the ODTS-modified SiO_2. In the saturation region ($V_d > V_g - V_t$), I_d can be described by the following equation:[60]

$$I_{ds} = \frac{WC_o\mu}{2L}(V_g - V_t)^2$$

Here W and L are channel width and length, respectively, C_o is the capacitance of gate insulator per unit area (SiO_2, 200 nm, C_0 = 17 nF/cm^2), μ is the hole mobility, and V_t is threshold voltage. The saturation-region mobility of the polymers was

dx.doi.org/10.1021/ma300313y | *Macromolecules* 2012, 45, 3047−3056

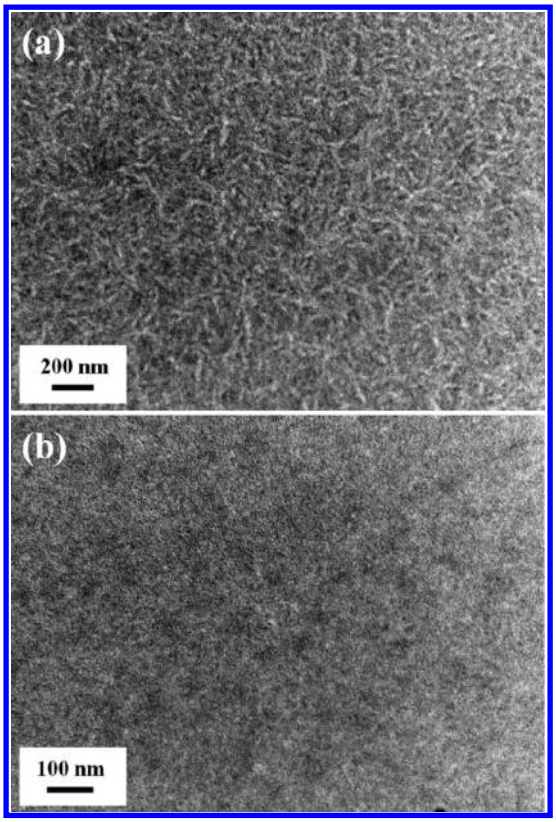

Figure 4. TEM images of (a) **P4TV** and (b) **P8TV** films prepared from *o*-dichlorobenzene solutions and annealed at 100 °C for 60 min.

calculated from the transfer characteristics of FET involving plotting $(I_d)^{1/2}$ versus V. As shown in Figure 6, the thermally annealed **P4TV** and **P8TV** reveal typical transfer and output curves. The FET mobilities of the annealed **P4TV** and **P8TV** thin films are $(1.24 \pm 0.20) \times 10^{-1}$ and $(1.79 \pm 0.25) \times 10^{-3}$ $cm^2\ V^{-1}\ s^{-1}$, with the current on-to-off ratio (I_{on}/I_{off}) in the range of 10^4–10^5. **P4TV** has a significantly higher carrier mobility than **P8TV**, due to the superior ordered morphology and more extended π–electron delocalization described previously. The high carrier mobility of **P4TV** is comparable to that of regioregular P3HT[22–24] and the other PTV derivatives (2.1×10^{-4} to 1.05 $cm^2\ V^{-1}\ s^{-1}$).[31–33]

The air stability of the devices were evaluated under ambient by measuring hole mobility (μ_h), on/off ratio (I_{on}/I_{off}), and threshold voltage (V_t) as a function of time, as shown in Figure 7 and Figure S6 (Supporting Information). As shown in the figure, both **P4TV** and **P8TV** exhibited relatively good air-stability. After exposure to air for 1 month, the hole mobility of **P4TV** decreased from 0.18 to 0.062 $cm^2\ V^{-1}\ s^{-1}$, which showed better air stability than P3HT attributed to the lower HOMO energy level. Note that P3HT exhibited a large degradation of charge mobility about 2 orders of magnitude when stored in air.[61] Compared to **P4TV**, the mobility of **P8TV** still kept around 0.0015 $cm^2\ V^{-1}\ s^{-1}$ even after exposure to air for 1 month. The outstanding air-stable performance of the **P8TV** may be correlated to its much low-lying HOMO energy level, avoiding the degradation and the doping of moisture and oxygen.

Polymer Photovoltaic Cell Characteristics. The bulk heterojunction photovoltaic (PV) cells were fabricated with a sandwich configuration of ITO/PEDOT:PSS/polymer:$PC_{71}BM$/Ca (30 nm)/Al (100 nm). The active layers of

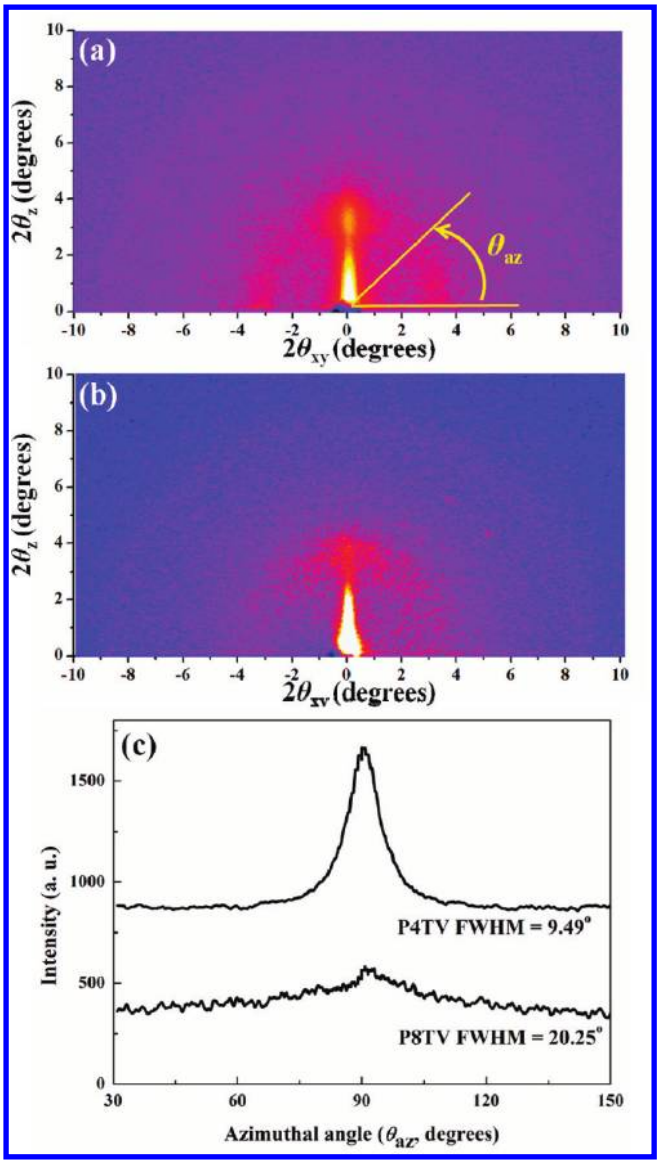

Figure 5. GIXD patterns of (a) **P4TV** film and (b) **P8TV** film prepared by spin coating on the ODTS-treated substrates from *o*-dichlorobenzene solutions and annealed at 100 °C for 60 min. (c) Azimuthal XRD profiles of the films at the first order diffraction in the θ_z direction.

the studied polymers devices were prepared through thermal annealing at 100 °C for 10 min. The J–V curves of polymer/$PC_{71}BM$ were measured under ambient after encapsulation with UV-curing glue, as shown in Figure 8. The PV characteristics, including open-circuit voltage (V_{oc}), short-circuit current (J_{sc}), fill factor (FF), and power conversion efficiency (PCE), of **P4TV** and **P8TV** devices are summarized in Table 2. The highest PCEs (%) of corresponding polymer-based PV devices are 4.04 (**P4TV**/$PC_{71}BM$ 1:1 w/w) and 2.69 (**P8TV**/$PC_{71}BM$ 1:2 w/w), respectively. The PCE of **P8TV**/$PC_{71}BM$ (1:1) device is only 1.74% relating to a lower FF as well as inferior film quality. The V_{oc} values of the **P4TV** and **P8TV**-based PV cells are 0.642 and 0.814 V, respectively. Obviously, the lower HOMO energy level of **P8TV** leads to a higher V_{oc} because the V_{oc} is related to the energy differences between the HOMO energy levels of the donor (conjugated polymers) and the LUMO energy levels of the acceptor

dx.doi.org/10.1021/ma300313y | *Macromolecules* 2012, 45, 3047–3056

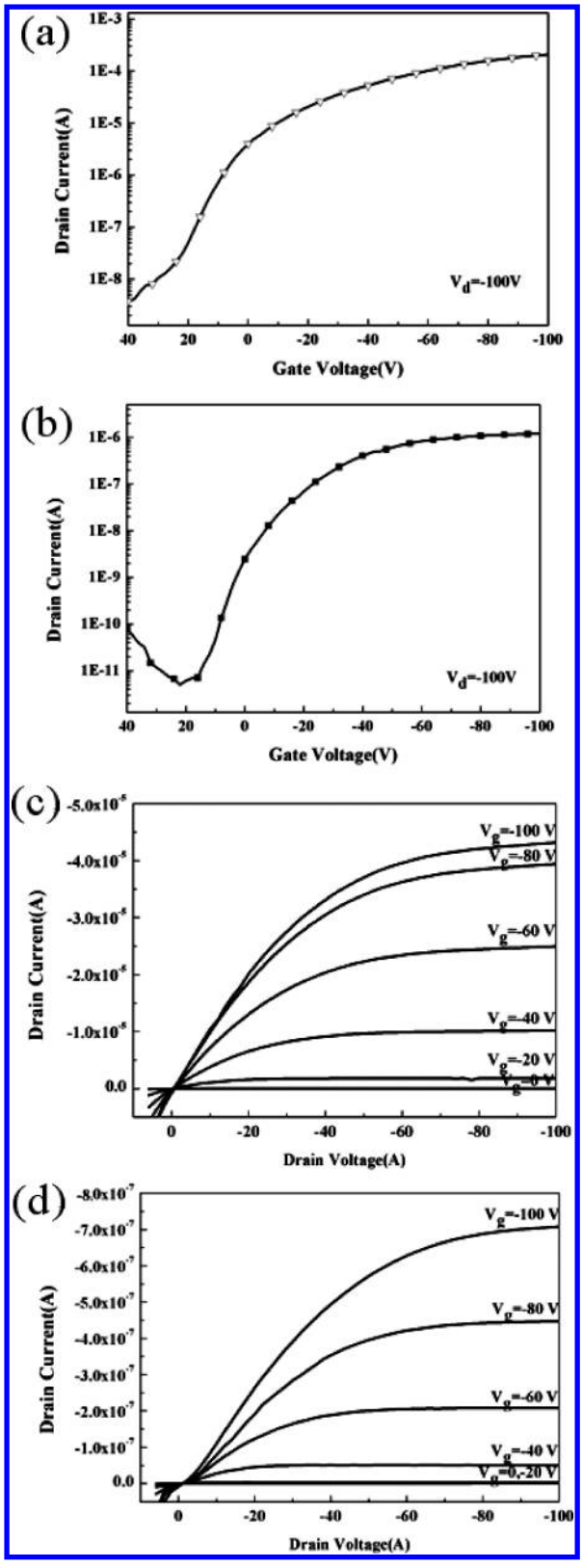

Figure 6. FET transfer characteristics of (a) **P4TV** and (b) **P8TV** thin films and the p-type output characteristics of (c) **P4TV** and (d) **P8TV**.

($PC_{71}BM$).[62] The J_{sc} values of these polymers are 11.689 mA/cm^2 (**P4TV**) and 6.709 mA/cm^2 (**P8TV**), respectively, which has the same trend as the hole FET mobility. Thus, the larger PCE of **P4TV** than **P8TV** is mainly due to the higher hole mobility (higher J_{sc}), and better absorption ability in visible

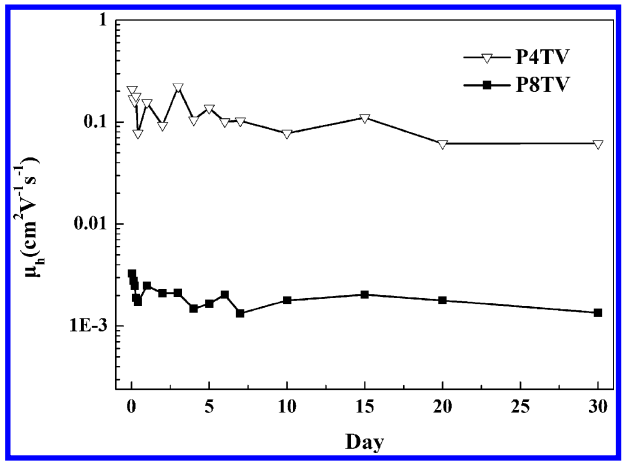

Figure 7. FET air-stability testing on the FET hole mobility of **P4TV** and **P8TV**-based devices. Relative humidity ranges from 41% to 60% in air.

light region. Furthermore, for **P4TV**, the J_{sc} is approximate 1.3 times larger than P3HT (9.097 mA/cm^2) and the smaller band gap increases the light absorption range, leading to better PCE characteristics than P3HT (3.86%) under the same processing condition.

The incident photon conversion efficiency (IPCE) curves of the PV cells based on **P4TV**, **P8TV**, and P3HT are demonstrated in Figure 8b. The IPCE curve of P3HT/$PC_{71}BM$ (1:1 w/w) device covers a wavelength range from 350 to 650 nm with the maximum IPCE value of 55% at ca. 570 nm. As compared to the P3HT device, **P8TV**/$PC_{71}BM$ (1:2) device shows a broader wavelength range from 350 to 700 nm, but the maximum IPCE value is only 41% at ca. 525 nm, thus causing the lower J_{sc} and PCE of **P8TV** device. For **P4TV**/$PC_{71}BM$ (1:1) device, the IPCE curve exhibits maximum IPCE value of 48% at ca. 625 nm, which is slightly lower than that of P3HT; however, it covers the broadest wavelength range from 350 to 750 nm and a platform from 450 to 700 nm. The longer absorption wavelength of **P4TV** device leads to the higher J_{sc} of the PV devices.

For bulk heterojunction PV cells, air stability is an issue as important as PCE. The diffusion of oxygen and moisture into the cells is generally regarded as the dominant source of degradation. It is necessary to extend the lifetime of devices by preventing the degradation from air and humidity. To explore the air stability for the lifetime of PV cells, the prepared devices with encapsulation were stored under an atmosphere with a relative humidity in a range of 60−80% and temperature at approximate 25 °C. As shown in Figure 8c, the PCE decays 22% in the case of P3HT/$PC_{71}BM$ (1:1) device after 40 days similar to our previous work.[26] However, **P4TV** and **P8TV** exhibited the degradation ratio of around 5−18% in the air for 40 days. The significantly enhanced environmental stability could be due to the lower HOMO levels than P3HT. For the blend of **P8TV**/$PC_{71}BM$, the $PC_{71}BM$ aggregations are smaller than 150 nm comparing to **P4TV**/$PC_{71}BM$ (larger than 250 nm) from TEM analysis (Figure S7 of the Supporting Information), which resulted in more stable device performance.[26] Note that the branched thiophene side chains could have better compatibility with $PC_{71}BM$.[39] Therefore, the PCE of the **P8TV**-based cells only decayed 5% after 40 days in air, due to the low-lying HOMO level and small $PC_{71}BM$ aggregation.

dx.doi.org/10.1021/ma300313y | *Macromolecules* 2012, 45, 3047−3056

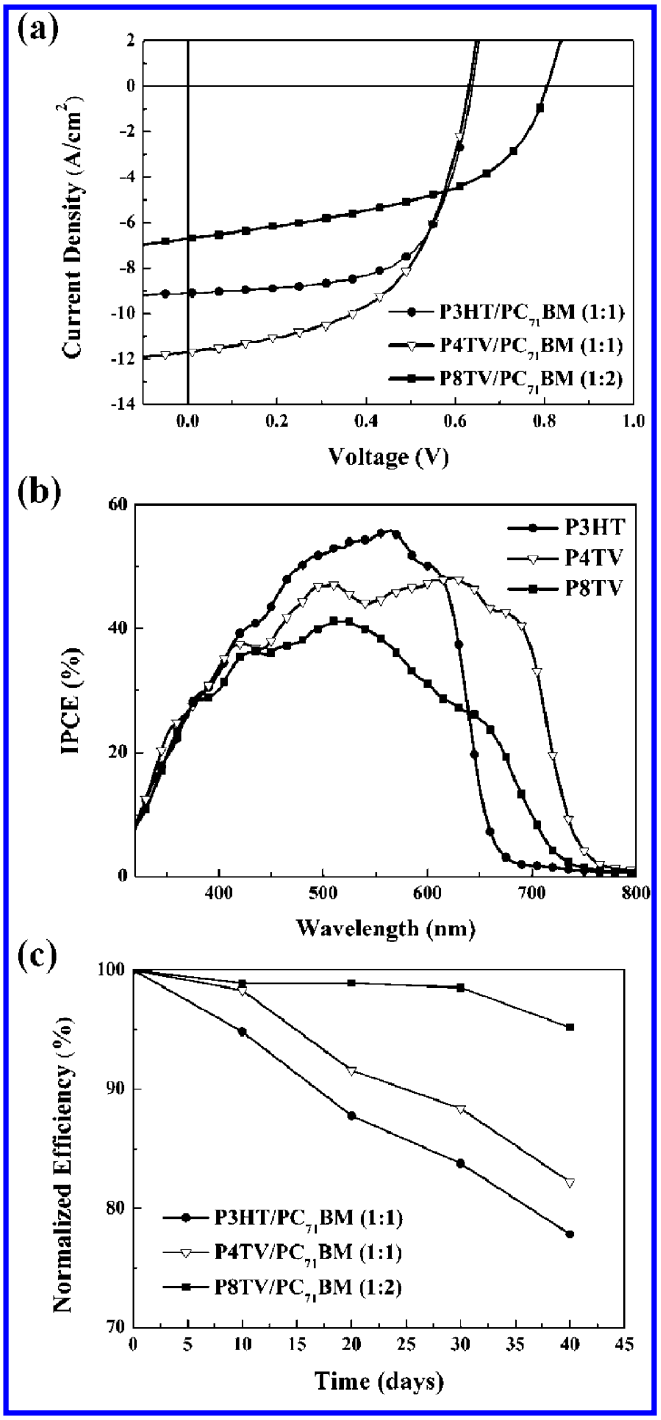

Figure 8. (a) *J*–*V* characteristics, (b) IPCE, and (c) air stability of polymer PV cells with the device structure of ITO/PEDOT:PSS/polymer:$PC_{71}BM$/Ca/Al.

Table 2. PV Characteristics with the Device Structure of ITO/PEDOT:PSS/Polymer:$PC_{71}BM$/Ca/Al Using P4TV, P8TV, and P3HT Processing from the DCB Solvent

polymer	polymer:$PC_{71}BM$	J_{sc} (mA/cm^2)	V_{oc} (V)	FF	PCE[a] (%)
P4TV	1:1	11.689	0.642	0.540	4.04
P8TV	1:1	5.867	0.819	0.362	1.74
P8TV	1:2	6.709	0.814	0.495	2.69
P3HT	1:1	9.097	0.634	0.633	3.68

[a]The average value of PCE is calculated from 4 pixels in the device.

CONCLUSIONS

We have successfully synthesized and characterized two new alternating copolymers containing vinylene moieties and biaxially extended quaterthiophene (**P4TV**) and octithiophene (**P8TV**) by the Pd-catalyzed Stille coupling reaction under microwave heating. The incorporation of vinylene moieties significantly reduced the conformation distortion in the main chain, leading to high coplanarity and the low band gaps of **P4TV** (1.69 eV) and **P8TV** (1.78 eV). Especially in the case of **P4TV**, high structural organization was observed in the GIXD and TEM analysis, mainly due to the reduction of conformation distortions and high coplanarity, resulting in high hole mobility of up to 0.12 cm^2 V^{-1} s^{-1}. **P8TV** with large side-chain torsional angles significantly exhibited the relatively lower mobility of 0.0018 cm^2 V^{-1} s^{-1}. The power conversion efficiencies (PCE) of the copolymers/$PC_{71}BM$ based photovoltaic cells were 4.04% (**P4TV**) and 2.69% (**P8TV**) under the illumination of AM 1.5G (100 mW/cm^2). They showed better PV cell performances than the PTV derivatives on account of their higher photocurrent and low-lying HOMO energy levels. Moreover, the outstanding environmental stability (decays 5% after 40 days in ambient) was observed from the **P8TV**-based PV devices owing to the low-lying HOMO energy level and small $PC_{71}BM$ aggregation. These above results reveal that new biaxially extended thiophene vinylene conjugated copolymers have the backbone coplanarity for increasing charge transport, photovoltaic properties, and air stability.

ASSOCIATED CONTENT

Supporting Information

Synthetic route and ^{1}H NMR spectrum of **8T-Br$_2$**, GPC traces of **P4TV** and **P8TV**, TGA curves and DSC curves of the studied copolymers at the heating rate of 10 °C/min under a nitrogen atmosphere, optical absorption spectra of **P4TV** and **P8TV** in dilute *o*-dichlorobenzene solutions, AFM phase images of **P4TV** and **P8TV** thin films, air-stability testing on the FET performance of **P4TV** and **P8TV**-based devices, including on/off ratio and threshold voltage with relative humidity ranges from 41% to 60% in air, and TEM images of blending films of **P4TV**/$PC_{71}BM$ (1:1, w/w) and **P8TV**/$PC_{71}BM$ (1:2, w/w). This material is available free of charge via the Internet at http://pubs.acs.org.

AUTHOR INFORMATION

Corresponding Author

*Telephone: 886-2-23628398. Fax: 886-2-23623040. E-mail: chenwc@ntu.edu.tw.

Author Contributions

†These authors contributed equally to this work

Notes

The authors declare no competing financial interest.

ACKNOWLEDGMENTS

The financial support from National Science Council of Taiwan is highly appreciated. We also acknowledge the helpful discuss with Prof. Ya-Sen Sun of National Central University of Taiwan.

REFERENCES

(1) Grimsdale, A. C.; Chan, K. L.; Martin, R. E.; Jokisz, P. G.; Holmes, A. B. *Chem. Rev.* **2009**, *109*, 897.
(2) Wu, W. C.; Liu, C. L.; Chen, W. C. *Polymer* **2006**, *47*, 527.

(3) Li, Y. N.; Wu, Y. L.; Liu, P.; Birau, M.; Pan, H. L.; Ong, B. S. *Adv. Mater.* **2006**, *18*, 3029.
(4) I, M.; Heeney, M.; Bailey, C.; Genevicius, K.; I, M.; Shkunov, M.; Sparrowe, D.; Tierney, S.; Wagner, R.; Zhang, W. M.; Chabinyc, M. L.; Kline, R. J.; Mcgehee, M. D.; Toney, M. F. *Nat. Mater.* **2006**, *5*, 328.
(5) Ong, B. S.; Wu, Y. L.; Liu, P.; Gardner, S. *Adv. Mater.* **2005**, *17*, 1141.
(6) Wu, Y. L.; Li, Y. N.; Ong, B. S.; Liu, P.; Gardner, S.; Chiang, B. *Adv. Mater.* **2005**, *17*, 184.
(7) Osaka, I.; McCullough, R. D. *Acc. Chem. Res.* **2008**, *41*, 1202.
(8) Lee, W. Y.; Cheng, K. F.; Wang, T. F.; Chueh, C. C.; Chen, W. C.; Tuan, C. S.; Lin, J. L. *Macromol. Chem. Phys.* **2007**, *208*, 1919.
(9) Li, G.; Shrotriya, V.; Huang, J. S.; Yao, Y.; Moriarty, T.; Emery, K.; Yang, Y. *Nat. Mater.* **2005**, *4*, 864.
(10) Liu, C. L.; Tsai, J. H.; Lee, W. Y.; Chen, W. C.; Jenekhe, S. A. *Macromolecules* **2008**, *41*, 6952.
(11) Thompson, B. C.; Frechet, J. M. J. *Angew. Chem. Inter. Ed.* **2008**, *47*, 58.
(12) Lai, M. H.; Chueh, C. C.; Chen, W. C.; Wu, J. L.; Chen, F. C. *J. Polym. Sci., Part A: Polym. Chem.* **2009**, *47*, 973.
(13) Park, S. H.; Roy, A.; Beaupre, S.; Cho, S.; Coates, N.; Moon, J. S.; Moses, D.; Leclerc, M.; Lee, K.; Heeger, A. J. *Nature Photo.* **2009**, *3*, 297.
(14) Tsai, J. H.; Chueh, C. C.; Lai, M.-H.; Wang, C. F.; Chen, W. C.; Ko, B. T.; Ting, C. *Macromolecules* **2009**, *42*, 1897.
(15) Liang, Y.; Xu, Z.; Xia, J.; Tsai, S.-T.; Wu, Y.; Li, G.; Ray, C.; Yu, L. *Adv.. Mater.* **2010**, *22*, E135.
(16) Tsai, J. H.; Chueh, C. C.; Chen, W. C.; Yu, C. Y.; Hwang, G. W.; Ting, C.; Chen, E. C.; Meng, H. F. *J. Polym. Sci., Part A: Polym. Chem.* **2010**, *48*, 2351.
(17) Brabec, C. J.; Heeney, M.; McCulloch, I.; Nelson, J. *Chem. Soc. Rev.* **2011**, *40*, 1185.
(18) Ling, Q. D.; Liaw, D. J.; Zhu, C.; Chan, D. S. H.; Kang, E. T.; Neoh, K.-G. *Prog. Polym. Sci.* **2008**, *33*, 917.
(19) Fang, Y. K.; Liu, C. L.; Li, C.; Lin, C. J.; Mezzenga, R.; Chen, W. C. *Adv. Funct. Mater.* **2010**, *20*, 3012.
(20) Kuorosawa, T.; Chueh, C. C.; Liu, C. L.; Higashihara, T.; Ueda, M.; Chen, W. C. *Macromolecules* **2010**, *43*, 1236.
(21) Ikegami, R.; Koresawa, A.; Shibata, T.; Takagi, K. *J. Org. Chem.* **2003**, *68*, 2195.
(22) Sirringhaus, H.; Brown, P. J.; Friend, R. H.; Nielsen, M. M.; Bechgaard, K.; Langeveld-Voss, B. M. W.; Spiering, A. J. H.; Janssen, R. A. J.; Meijer, E. W.; Herwig, P.; de Leeuw, D. M. *Nature* **1999**, *401*, 685.
(23) Wang, G. M.; Swensen, J.; Moses, D.; Heeger, A. J. *J. Appl. Phys.* **2003**, *93*, 6137.
(24) Bao, Z.; Dodabalapur, A.; Lovinger, A. J. *Appl. Phys. Lett.* **1996**, *69*, 4108.
(25) Li, G.; Yao, Y.; Yang, H.; Shrotriya, V.; Yang, G.; Yang, Y. *Adv. Funct. Mater.* **2007**, *17*, 1636.
(26) Tsai, J. H.; Lai, Y. C.; Higashihara, T.; Lin, C. J.; Ueda, M.; Chen, W. C. *Macromolecules* **2010**, *43*, 6085.
(27) Yang, X. N.; Loos, J.; Veenstra, S. C.; Verhees, W. J. H.; Wienk, M. M.; Kroon, J. M.; Michels, M. A. J.; Janssen, R. A. J. *Nano Lett.* **2005**, *5*, 579.
(28) Yu, C. Y.; Ko, B. T.; Ting, C.; Chen, C. P. *Sol. Energy Mater. Sol. Cells* **2009**, *93*, 613.
(29) Eckhardt, H.; Shacklette, L. W.; Jen, K. Y.; Elsenbaumer, R. L. *J. Chem. Phys.* **1989**, *91*, 1303.
(30) Henckens, A.; Knipper, M.; Polec, I.; Manca, J.; Lutsen, L.; Vanderzande, D. *Thin Solid Films* **2004**, *451*, 572.
(31) Lim, B.; Baeg, K. J.; Jeong, H. G.; Jo, J.; Kim, H.; Park, J. W.; Noh, Y. Y.; Vak, D.; Park, J. H.; Park, J. W.; Kim, D. Y. *Adv. Mater.* **2009**, *21*, 2808.
(32) He, Y. J.; Wu, W. P.; Zhao, G. J.; Liu, Y. Q.; Li, Y. F. *Macromolecules* **2008**, *41*, 9760.
(33) Jang, S. Y.; Lim, B.; Yu, B. K.; Kim, J.; Baeg, K. J.; Khim, D.; Kim, D. Y. *J. Mater. Chem.* **2011**, *21*, 11822.
(34) Wu, P. T.; Kim, F. S.; Jenekhe, S. A. *Chem. Mater.* **2011**, *23*, 4618.
(35) Chueh, C. C.; Lai, M. H.; Tsai, J. H.; Wang, C. F.; Chen, W. C. *J. Polym. Sci., Part A: Polym. Chem.* **2010**, *48*, 74.
(36) Kim, J.; Lim, B.; Baeg, K. J.; Noh, Y. Y.; Khim, D.; Jeong, H. G.; Yun, J. M.; Kim, D. Y. *Chem. Mater.* **2011**, *23*, 4663.
(37) Smith, A. P.; Smith, R. R.; Taylor, B. E.; Durstock, M. F. *Chem. Mater.* **2004**, *16*, 4687.
(38) Li, Y. F.; Zou, Y. P. *Adv. Mater.* **2008**, *20*, 2952.
(39) Zhou, E. J.; Tan, Z. A.; Huo, L. J.; He, Y. J.; Yang, C. H.; Li, Y. F. *J. Phys. Chem. B* **2006**, *110*, 26062.
(40) Hou, J. H.; Tan, Z. A.; Yan, Y.; He, Y. J.; Yang, C. H.; Li, Y. F. *J. Am. Chem. Soc.* **2006**, *128*, 4911.
(41) Hou, J. H.; Huo, L. J.; He, C.; Yang, C. H.; Li, Y. F. *Macromolecules* **2006**, *39*, 594.
(42) Hou, J. H.; Yang, C. H.; He, C.; Li, Y. F. *Chem. Commun.* **2006**, 871.
(43) Tsai, J. H.; Lee, W. Y.; Chen, W. C.; Yu, C. Y.; Hwang, G. W.; Ting, C. *Chem. Mater.* **2010**, *22*, 3290.
(44) Lin, C. J.; Lee, W. Y.; Lu, C.; Lin, H. W.; Chen, W. C. *Macromolecules* **2011**, *44*, 9565.
(45) Lin, H.-W.; Lee, W.-Y.; Lu, C.; Lin, C.-J.; Wu, H.-C.; Lin, Y.-W.; Ahn, B.; Rho, Y.; Ree, M.; Chen, W.-C. *Polym. Chem.* **2012**, *3*, 767.
(46) Chang, Y. T.; Hsu, S. L.; Chen, G. Y.; Su, M. H.; Singh, T. A.; Diau, E. W. G.; Wei, K. H. *Adv. Funct. Mater.* **2008**, *18*, 2356.
(47) Chang, Y. T.; Hsu, S. L.; Su, M. H.; Wei, K. H. *Adv. Mater.* **2009**, *21*, 2093.
(48) Zou, Y. P.; Wu, W. P.; Sang, G. Y.; Yang, Y.; Liu, Y. Q.; Li, Y. F. *Macromolecules* **2007**, *40*, 7231.
(49) Zen, A.; Bilge, A.; Galbrecht, F.; Alle, R.; Meerholz, K.; Grenzer, J.; Neher, D.; Scherf, U.; Farrell, T. *J. Am. Chem. Soc.* **2006**, *128*, 3914.
(50) Sun, X. B.; Liu, Y. Q.; Chen, S. Y.; Qiu, W. F.; Yu, G.; Ma, Y. Q.; Qi, T.; Zhang, H. J.; Xu, X. J.; Zhu, D. B. *Adv. Funct. Mater.* **2006**, *16*, 917.
(51) Shang, H. X.; Fan, H. J.; Liu, Y.; Hu, W. P.; Li, Y. F.; Zhan, X. W. *J. Mater. Chem.* **2011**, *21*, 9667.
(52) Kanibolotsky, A. L.; Perepichka, I. F.; Skabara, P. J. *Chem. Soc. Rev.* **2010**, *39*, 2695.
(53) Rance, W. L.; Rupert, B. L.; Mitchell, W. J.; Kose, M. E.; Ginley, D. S.; Shaheen, S. E.; Rumbles, G.; Kopidakis, N. *J. Phys. Chem. C* **2010**, *114*, 22269.
(54) Ma, C. Q.; Fonrodona, M.; Schikora, M. C.; Wienk, M. M.; Janssen, R. A. J.; Bauerle, P. *Adv. Funct. Mater.* **2008**, *18*, 3323.
(55) Frisch, M. J.; Trucks, G. W.; Schlegel, H. B.; Scuseria, G. E.; Robb, M. A.; Cheeseman, J. R.; Montgomery, J., J. A.; Vreven, T.; Kudin, K. N.; Burant, J. C.; Millam, J. M.; Iyengar, S. S.; Tomasi, J.; Barone, V.; Mennucci, B.; Cossi, M.; Scalmani, G.; Rega, N.; Petersson, G. A.; Nakatsuji, H.; Hada, M.; Ehara, M.; Toyota, K.; Fukuda, R.; Hasegawa, J.; Ishida, M.; Nakajima, T.; Honda, Y.; Kitao, O.; Nakai, H.; Klene, M.; Li, X.; Knox, J. E.; Hratchian, H. P.; Cross, J. B.; Bakken, V.; Adamo, C.; Jaramillo, J.; Gomperts, R.; Stratmann, R. E.; Yazyev, O.; Austin, A. J.; Cammi, R.; Pomelli, C.; Ochterski, J. W.; Ayala, P. Y.; Morokuma, K.; Voth, G. A.; Salvador, P.; Dannenberg, J. J.; Zakrzewski, V. G.; Dapprich, S.; Daniels, A. D.; Strain, M. C.; Farkas, O.; Malick, D. K.; Rabuck, A. D.; Raghavachari, K.; Foresman, J. B.; Ortiz, J. V.; Cui, Q.; Baboul, A. G.; Clifford, S.; Cioslowski, J.; Stefanov, B. B.; Liu, G.; Liashenko, A.; Piskorz, P.; Komaromi, I.; Martin, R. L.; Fox, D. J.; Keith, T.; Al-Laham, M. A.; Peng, C. Y.; Nanayakkara, A.; Challacombe, M.; Gill, P. M. W.; Johnson, B.; Chen, W.; Wong, M. W.; Gonzalez, C.; Pople, J. A. *Gaussian 03, revision B.04*; Gaussian, Inc.: Wallingford, CT, 2004.
(56) Operamolla, A.; Farinola, G. M. *Eur. J. Org. Chem.* **2011**, *2011*, 423.
(57) Yu, C. Y.; Chen, C. P.; Chan, S. H.; Hwang, G. W.; Ting, C. *Chem. Mater.* **2009**, *21*, 3262.
(58) Yang, H. C.; Shin, T. J.; Yang, L.; Cho, K.; Ryu, C. Y.; Bao, Z. N. *Adv. Funct. Mater.* **2005**, *15*, 671.
(59) Qiu, L.; Lee, W. H.; Wang, X.; Kim, J. S.; Lim, J. A.; Kwak, D.; Lee, S.; Cho, K. *Adv. Mater.* **2009**, *21*, 1349.

(60) Zaumseil, J.; Friend, R. H.; Sirringhaus, H. *Nat. Mater.* **2005**, *5*, 69.
(61) Schafferhans, J.; Baumann, A.; Deibel, C.; Dyakonov, V. *Appl. Phys. Lett.* **2008**, *93*, 093303.
(62) Gadisa, A.; Svensson, M.; Andersson, M. R.; Inganas, O. *Appl. Phys. Lett.* **2004**, *84*, 1609.